Promote Scientific Research is Our Way to Serve the Community

Graphene Oxide and Graphene functionalized artificial sweetener (Saccharine): Novel Syntheses, Characterization and Comparative study of their electrical properties

Firas S. Abdulazeez , Ibtehal Q. Abdulah , Mustafa A.Ulghafoor
Department of Chemistry, College of Science, Tikrit University, Tikrit, Iraq

ARTICLE INFO.

Keywords: Graphene Oxide (GO); Graphene (G); Saccharine (Sac); GO-Sac; G-Sac; XRD; AFM; LCR measurements.

Name: **Firas S. Abdulazeez**
E-mail:
Tel:

ABSTRACT

Two carbon nanostructures; graphene oxide (GO) and graphene (G) were synthesized and characterized with a view to study their electrical properties after functionalization with saccharine. After preparation acyl chloride of graphene oxide, saccharine was mainly covalently linked to graphene oxide nanostructure with formation of amide bond afforded GO-Sac, while it was physically linked to graphene nanosheets with formation of G-Sac. These two saccharine nano derivatives were characterized using FT-IR, powder X-ray diffraction (XRD) and atomic force microscope (AFM) techniques. Herein, saccharine not only used for enhance the electrical properties of GO or G but it was played a main role in increasing of the distance between graphene (G) and graphene oxide (GO) sheets, and consequently prevent the agglomeration effect on graphene oxide and graphene sheets. The electrical properties of these materials were measured using inductance, capacitance, and resistance measurements (LCR). The results showed increased electrical properties of both two carbon nanostructures with enhance their electrical storage after treating with saccharine.

Introduction

Scientists have realized only graphite and diamond allotropes of carbon two hundred years ago [1]. Nowadays, more than five allotropes of carbon nanostructures were discovered. The most attractive allotropes are graphene oxide and graphene which are extensively studied and used owing to graphene oxide- and graphene-containing nanomaterials fantastic electrical in G only [2,3],optical [4,5], thermal [6,7], mechanical [8,9], biological [10,11] and catalytic [12,13] properties. In the case of GO, these intriguing and unique properties are due to its polymeric nanostructure which provide high surface area [14], but the most important reason is the possession of many oxygenic functional groups that are carboxyl, hydroxyl in addition to epoxy groups [14-17]. While in the case of G, the distinctive electrical or other properties are due its unique structure that has SP^2-C atoms with pi conjugated system that and some of oxygenic functional groups that found due to incompletely chemically reduction of GO by hydrazine [18].

The chemical compounds that have at least one active site able to react with carboxyl groups on GO via condensation reaction are either covalently bonded with COOH and/or OH in addition to non-covalently with Pi-Pi stacking (electrostatically) and / or hydrogen bonding [19], while these compounds are non-covalently liked to fully reduced GO. Therefore enhancement of the surface of GO and G via chemical reaction was studied [19-26] while G sheet prepared via hydrazine reduction of GO, has excellent electrical conductivity because the chemically reduction of GO can eliminate a significant quantity of oxygenic functional groups and lead to G sheets with low functional-group content. Whereas GO nanosheets can easily chemically modified with different compounds, its electrical properties can be enhanced only after thermal annealing, which probably converts GO into G [27]. Unfortunately, this thermal method degrades GO structural integrity. Therefore in this article we tried to use one of most common sweeteners (saccharine) for modification of

graphene oxide and graphene in order to show the effect of saccharine on their electrical properties.

Experimental

Materials

Graphite flakes with an average particle size of 300 mesh (>%99) were purchased from Qingdao-Guangyao Graphite Co.Ltd. (China). Polyvinylalcohol (PVA) Sulfuric acid (H_2SO_4, 98%), sodium nitrate ($NaNO_3$,99%), hydrochloric acid (HCl,37%), potassium permanganate ($KMnO_4$,99%), hydrogen peroxide (H_2O_2,30%), hydrazine monohydrate ($N_2H_4.H_2O$, 50-60%), Sodium saccharinate ($C_7H_4NO_3SNa$, 99.%) and were purchased from Merck & Co (Germany). These chemicals were used without further treatment or purification except dimethylformamide (DMF, 98%) and thionylchloride ($SOCl_2$, 97%) which were purchased from Sigma-Aldrich (UK) purified by low pressure distillation.

Instrumentation

All infrared spectra of nanomaterials were measured in SHIMADZU8400S spectrophotometer at a range 400-4000 cm^{-1} as KBr discs, powder X-ray diffraction measurements were measured

Using (Shimadzu XR6000) device with Nickel - Copper filter (CuKα,λ= 1.5406 Å), Atomic force microscope images (AFM) were pictured using atomic force microscope type PHYW. Electrical test device was measured using Hewlett Packard LCR device, where; Inductance(L), Capacitance(C) and Resistance (R).

Methods

Preparation of graphene oxide (GO)

Graphite oxide was synthesized according to a modified Hummers' method [28]. A graphite powder (300 mesh) (0.1 g) was added to cool concentrated H_2SO_4 (7 mL) in the three-neck flask and left to stir uniformly in an ice bath for 15 mins. A fine mixture of sodium nitrate (0.4 g) and potassium permanganate (0.6 g) were added carefully to above mixture and stirred in an ice bath for 2 h. The ice-bath was then removed and the temperature of the mixture was kept at 35°C in water path for 30 mins. The mixture was converted to a pasty (brown in color). Deionized water (5 mL) was added to the mixture and the temperature was then raised to 90-98 ^oC . The above mixture was diluted by warm deionized water (25 mL). After that, 30% H_2O_2 (~ 5 ml) was added till the solution turned to bright yellow. The graphitic oxide powder was dried under vaccume at 40 ^oC for 4 h. Graphitic oxide (0.1 g) in deionized water (40 mL) was then dispersed by ultrasonic to give graphene oxide nanosheets.

Preparation of graphene (G) [29]

The Prepared graphene oxide nanosheet (GO) (0.5 g) was dispersed in deionized water (100mL) under ultrasonic treatment for half an hour and the resulted bright yellow dispersion was then treated with $N_2H_4.H_2O$. Black precipitate was immediately formed and then heated at 80 ^oC for 20 h. The resulted mixture were centrifuged at 5000rpm, washed out with deionized water for three times and dried at 70 ^oC for 4 h providing a black powder of graphene.

Preparation of graphene oxide acyl chloride (GO-CO-Cl) and (GO-Sac)

The Prepared graphene oxide oxide nanosheet (GO) (0.2 g) was dispersed in DMF (3mL) under ultrasonic treatment for 1h and was then treated with $SOCl_2$ and heated at 75 ^oC for 24 h under inert atmosphere (N_2). The volatile fractions were evaporated in vacuum at low pressure, DMF(40 mL), sodium saccharinate (5.0 g) and triethyl amine (0.5 mL) were added to the residue at 5^oC for 20 h. The resulted mixture was centrifuged at 5000 rpm for 5 mins. and washed out with deionized water for ten times providing a grayish-black powder of GO that chemically functionalized by saccharine. See Scheme 1 and Fig. 1(a) for 3D viewing.

Preparation of (G-Sac)

The Prepared graphene oxide nanosheet (GO) (0.4 g) was dispersed in DMF (30mL) under ultrasonic treatment for 1h and was then treated with sodium saccharinate (10 g) and refluxed at 75 ^oC for 40 h. The resulted mixture was centrifuged at 5000 rpm for 5 mins. and washed with deionized water for ten times providing a black powder of G that physically functionalized by saccharine. Scheme 1 and Fig. 1(b) for 3D viewing.

Preparation of a thin films

The PVA powder was firstly dissolved in the smallest amount of water and was then doped with the prepared nanomaterials with a weight ratio of only 5%. The mixture was then subjected to ultrasound for two hours to obtain a homogeneous mixture and then poured into 4 cm molds and left to dry for two days at temperature room.

LCR Calculations

The real electrical permittivity constant represents energy conservation in the material when exposed to an electric field [30] and it can be calculated by the following equation:

$\varepsilon_R=(C\ d)/(\varepsilon_o\ A)$, Where; ε_R is a real permittivity, C is a capacitance, d is a film thickness, ε_o is the vacuum isolation constant 10-12 x 8.85 $F.m^{-1}$ and A is the electrode area which equal 1 cm.

The imaginary electrical permittivity constant is a quantity of electrical energy that turns over time into thermal energy, which is not a good factor for the materials that invest in the field of electric storage, the more the value of ε_R the material the less conservation of electrical energy. Th imaginary permittivity constant can be calculated by the following equation [31].

$\varepsilon_I= \tan\delta.\varepsilon_R$ Where; ε_I is an imaginary permittivity, $\tan\delta$ is a constant represents loss energy factor and ε_R is a real permittivity.

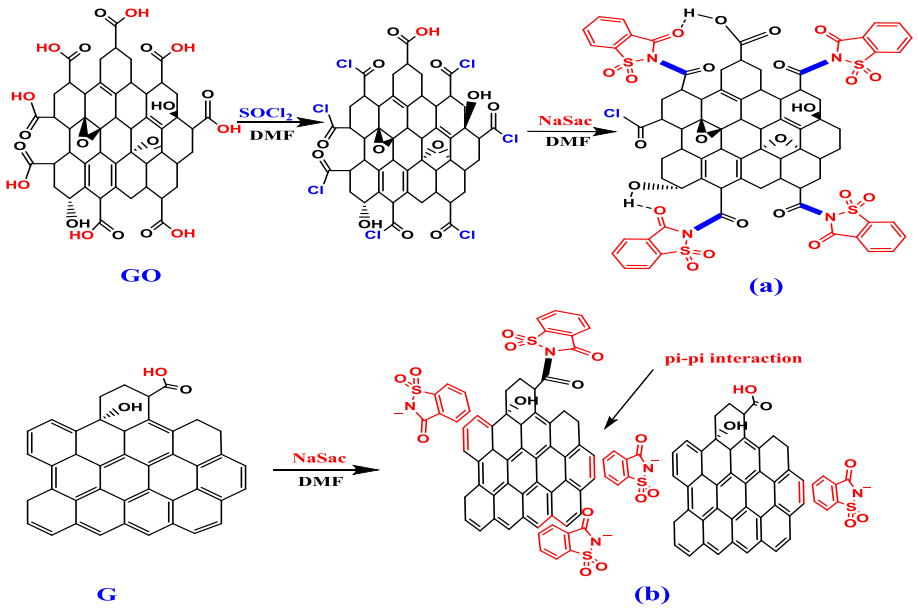

Scheme1. Schematic illustration for the preparation pathways of: (a)GO-Sac and (b) G-Sac.

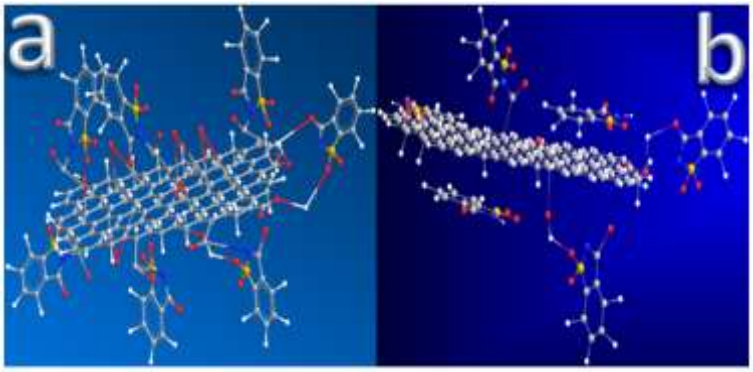

Fig. 1. 3D view of (a)GO-Sac and (b) G-Sac

Results and discussion

FTIR characterization

The investigation in the FT-IR spectrum of graphene oxide Fig. 2(a) shows eight main peaks at: 3431, 2928, 2864, 1718, 1653, 1381, 1200 and 1128cm^{-1} for the vibration modes of ν(OH), symmetric ν(CH_2), anti-symmetric ν(CH_2), ν(C=O), ν(C=C) of un-oxidized graphite domain,ν(C-O) of carboxylic acid, ν(C-O) of epoxy and alkoxy groups respectively [19,32].

In the case of FT-IR spectrum of graphene nanosheets Fig. 2(b), there are only three main intense peaks. The vibration modes of ν(H-C=C) appears at 3020 cm^{-1} while both 1640 and 1540 cm^{-1} attributes to ν(C=C) that formed after de-oxygenation the C-C containing carbonyl, epoxy or hydroxyl groups which is associated with transformation of C-SP^3 into C-SP^2[33]. The other weak-intense peaks represented to the remnant of un-reduced group of GO.

The FT-IR spectrum of functionalized graphene oxide (GO-Sac) Fig. 2(c) shows many peaks at 3095 cm^{-1} of ν(H-C=C,Sac), 2972 cm^{-1} of ν(H-C-C,GO), 1749 cm^{-1} of ν(C=O,GO), 1647 cm^{-1} of ν(H-C-C,Sac), 1629, 1587 cm^{-1} of ν(C=C,Sac), 1448 cm^{-1} of ν(C-N,Sac), 1336 cm^{-1} of ν(C-O,GO) and 1255 cm^{-1} of νasym(SO_2,Sac), 1178 cm^{-1} of νsym(SO_2,Sac). In this spectrum it can be note that the peak at 3446 cm^{-1} of ν(OH,GO) spectrum Fig. 2(a) was disappeared which improves the saccharine anion reacted and attached successfully to GO via condensation reaction. Another evidence for occurrence of this reaction comes from the lower shifting of ν(C-N,Sac) from 1460 in free molecule 34] to 1448 cm^{-1} after reaction with GO.

The FT-IR spectrum of functionalized graphene (G-Sac) Fig. 2(d) shows many broad saccharine peaks at 3065,3005cm^{-1} of ν(H-C=C,Sac), 1654 cm^{-1} of ν(C=O ,Sac and C=C, G), 1537 cm^{-1} of ν(C=C,Sac), 1460 cm^{-1} of ν(C-N,Sac), 1359 cm^{-1} of ν(C-O,Sac). The evidence for this reaction derives from the simple FT-IR spectrum of this molecule which is more simple than free saccharine spectrum with very little changes in their shifting. These assignments can be attributed to the physical linking (pi-pi stacking) of saccharine onto the surface of G which contains undesirable functional group as could be seen in Scheme 1 and Fig.1(b).

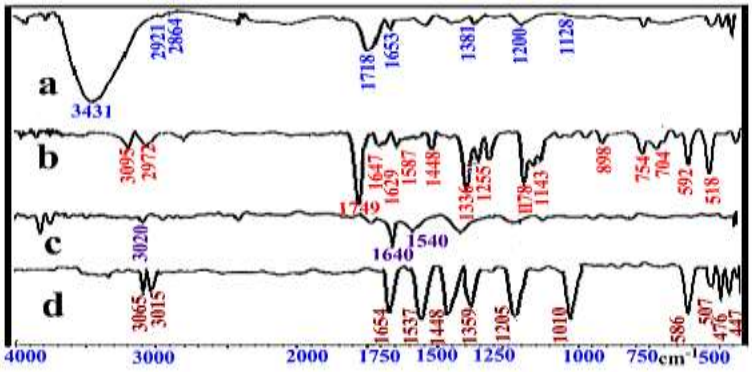

Fig. 2. FTIR spectra of (a)GO, (b) GO-Sac, (c) G, and (d) G-Sac

AFM characterization

The morphology of the GO-Sac was pictured and measured using AFM Fig.3(a-c),Table1. The maximum height of GO-Sac was 6.21 nm with smooth sheets-shaped in appearance as illustrated in the 3D-AFM image in Fig.3(a). The length of the chose sheet in Fig.3 was calculated depends on the section area analyses in Fig.3(b) and the result shows that the length was 1.4 µm with maximum fold height not exceed 0.6 nm while the thickness of the middle sheet was measured depends on the section area analyses in Fig.3 (c) and result shows that the thickness of the chose sheet was 1.7 nm. These results meant and prove the excellent conditions (5°C, 20 h in NEt_3) used to prepare big length sheets with very fine thickness with no aggregations which prevented by the saccharine molecules.

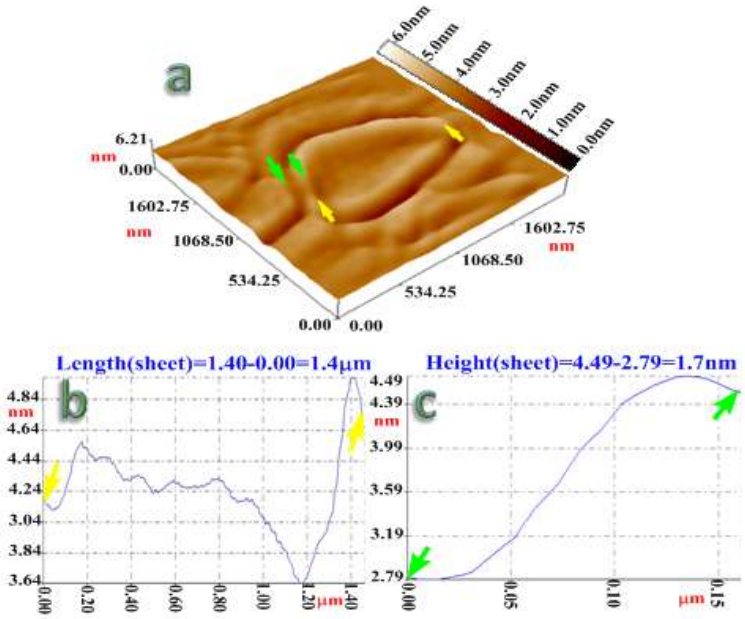

Fig.3. AFM results of GO-Sac; (a) 3D-image, (b) the section area of length of sheet and (c) the section area of thickness of sheet.

The morphology of the G-Sac was pictured and measured using AFM Fig.4(a-c). The maximum height of G-Sac was 6.21 nm with smooth folded sheet-shaped in appearance as illustrated in the 3D-AFM image in Fig.4(a). The length of the chose folded-sheet in Fig.4 was calculated depends on the section area analyses in Fig.4(b) and the result shows that the length was 1.6 µm with fold height not exceed 0.3 nm while the thickness of the middle sheet was measured depends on the section area analyses in Fig.4 (c) and result shows that the thickness of the chose sheet was 1.6 nm. These results meant and prove the excellent conditions used to prepare folded sheets with very fine thickness and no aggregations which prevented by the saccharine molecules.

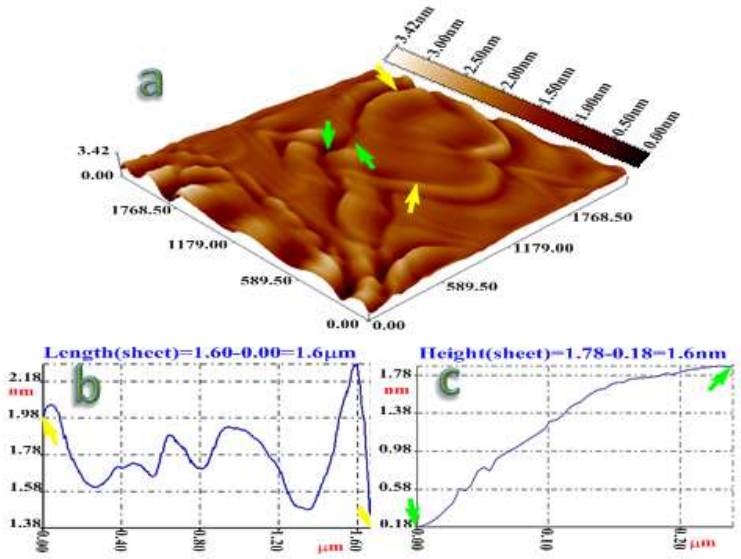

Fig.4. AFM results of G-Sac; (a) 3D-image, (b) the section area analyses of length of sheet and (c) the section area analyses of thickness of sheet.

X-ray diffraction measurements

XRD pattern of GO nanosheets obtained by chemical oxidation of graphite flakes shows in Fig.5(a). There are only two main peaks at (2θ) 11.9004° *(characteristic peak)* and 25.4998° with inter planar spacing 7.710 and 3.4910 Å [10,19]. XRD pattern of G nanosheets obtained by chemical reduction of GO shows two broad peak at 24.8801° *(characteristic peak)* and 43.3299° with inter planar spacing 3.5402 and 3.800 Å and this assignment in agreement with the XRD pattern of G[35]. XRD pattern of GO-Sac nanosheets obtained via condensation reaction gives five main peaks while the XRD pattern of G-Sac nanosheets shows only four main peaks listed in Table 1. The GO-Sac measurement Fig. 5(c) showed the disappearance of the main peak at (2θ) 11.9004° of GO, indicating the reduction of GO by saccharine and considered a main evidence for covalent link between GO and Sac molecules. However, it can be clearly showed that, both XRD of GO-Sac Fig.5(c) and G-Sac Fig.5(d) are approximately similar in the 2θ range 30-50° except for the possession of GO-Sac strong peak at (2θ) 23.1402° *(characteristic peak)*. This assignment considers a good evidence for the different linking between Sac and GO or G, so the (2θ) 23.1402° is represents the covalent bonds between GO and Sac. The XRD pattern of G-Sac Fig. 5(d) also shows the disappearance the characteristic peak of G at (2θ) 24.8801° due to the pi-pi stacking interaction of Sac with the skeletal C=C bonds of G and this give new *(characteristic peak)* at (2θ) 15.7661°. It should be mention that the intensity of saccharine peaks in GO-Sac are less than the intensities in G-Sac and this assignment due to high ability of GO to react with Sac molecules than G because of GO contains many functional groups able to react chemically or physically with saccharine while in the case of G only electrostatically bonds and very little number of functional groups are able to react and link to saccharine. Depending on Debye-Scherrer equation[36], $Dc = K\lambda/\beta\cos\theta$, where; β=breadth of the experimental diffraction line at half of the maximum intensity maximum, K=shape factor constant= 0.9 and λ wavelength of X-ray source, the average crystallite diameter (Dc) of GO, G, GO-Sac and G-Sac were approximately 10.4, 8.50, 30.32 and 28.59 nm respectively, Table 1.

Fig.5. XRD pattern of (a) GO, (b) G, (C) GO-Sac, (d) G-Sac. Where; blue ball represents characteristic peak

Table 1. XRD and AFM results of the prepared nanomaterials

Material	XRD					AFM			
	2θ (o)	d(Å)	FWHM (o)	D(nm)	D av. (nm)	Fold Height (nm)	Thickness (nm)	Length (μm)	Max Height (nm)
GO-Sac	15.5185	5.7054	0.2900	28.889	30.321	0.6	1.7	1.4	6.21
	23.1402	3.8406	0.2691	31.490					
	25.9144	3.4354	0.2366	36.000					
	27.8079	3.2056	0.3081	27.760					
	28.8089	3.0965	0.3120	27.470					
G-Sac	15.7661	5.6165	0.3267	25.650	28.590	0.3	1.6	1.6	3.42
	26.6731	3.3394	0.2700	31.600					
	29.6478	3.0107	0.2880	29.82					
	30.1606	2.9607	0.3150	27.29					

Electrical properties of nanomaterials

In the conductivity measurements, we observed that the addition of the saccharine improved the electrical properties of the graphene oxide. This observation comes from the highest value of conductivity which was 2.06E-18 whilst found to be 2.41E+00 in the GO-Sac. This is consistent with the partial reduction of the graphene oxide observed in the X-ray measurement and this reduction is accompanied by the transformation of part of the single bonds into double bonds and therefore the electronic density will increase as a result of electron retention within the pi system for a longer period. However, the graphene conductivity was better than that obtained in the two compounds containing the saccharine. The measurements showed that the highest value was measured for graphene to be 4.32E+01 while the G-Sac was 8.12E+00. Thus, we can arrange the synthesized materials according to their conductivity in the following sequence; G > G-Sac > GO-Sac > GO. All these values were illustrated in Table 2.

Table 2. The conductivity values of the prepared nanomaterials

σ GO	σ GO-Sac	σ G	σ G-Sac	Log Hz
1.05E-19	2.41E+00	4.32E+01	5.32E+00	4.310845
1.39E-19	1.23E+00	2.33E+01	5.33E+00	4.611344
2.11E-19	1.28E+00	2.14E+01	6.14E+00	4.787258
3.49E-19	1.29E+00	2.07E+01	7.07E+00	4.912108
2.33E-19	1.31E+00	2.00E+01	7.00E+00	5.008965
9.72E-19	1.25E+00	1.90E+01	7.40E+00	5.088111
1.25E-19	1.24E+00	1.82E+01	7.82E+00	5.155032
2.71E-20	1.18E+00	1.71E+01	7.71E+00	5.213005
3.31E-20	1.26E+00	1.81E+01	7.81E+00	5.264143
2.06E-18	1.26E+00	1.77E+01	7.77E+00	5.309889
5.20E-19	2.41E+00	9.32E+00	8.12E+00	5.351272

The relation of permittivity with frequency in the range (20457.14-224528.6 Hz) for the PVA films contained 5% pure G, pure GO, GO-Sac, and G-Sac were measured respectively, to study their electrical properties after and before functionalization with one of the artificial sweeteners saccharine.

At low frequencies permittivity, attained higher values, in all cases, then drop rapidly with increasing of frequencies as in Table 3. This assignment considered good improvement for conductivity-frequency dependence, due charge migration via the whopping mechanism [19,37]. The materials that have a higher value of (ƐR) and lower value of (ƐI) could increase the electrical storage [19]. In this study, the functionalization of GO with saccharine possessed a relatively highly (ƐR) and (ϭ) with low (ƐI), as shown in Tables 3 while with graphene, the addition of the saccharine decreases conductivity but enhanced the electrical storage via decreasing imaginary permittivity and arise real permittivity.

Table 3. Dielectric constants values of the prepared nanomaterials

$Ɛ_R$ GO	$Ɛ_R$GO-Sac	$Ɛ_I$GO	$Ɛ_I$GO-Sac	$Ɛ_R$G	$Ɛ_R$G-Sac	$Ɛ_I$G	$Ɛ_I$G-Sac	Log Hz
5.14E-25	2.43E+00	2.18E-05	3.35E-13	2.00E+01	2.37E+01	4.871490	5.010297	4.310845
4.99E-25	2.22E+00	2.72E-05	3.35E-13	2.02E+01	2.15E+01	3.850000	3.751198	4.611344
4.79E-25	2.28E+00	1.39E-05	3.40E-13	2.00E+01	2.12E+01	3.611101	2.626872	4.787258
4.04E-25	2.29E+00	1.45E-05	3.41E-13	2.11E+01	2.08E+01	3.015542	2.416183	4.912108
4.05E-25	2.24E+00	1.45E-05	3.42E-13	2.15E+01	2.05E+01	2.551702	2.339204	5.008965
3.25E-25	2.23E+00	1.48E-05	3.23E-13	2.13E+01	2.02E+01	2.522230	2.256395	5.088111
3.31E-25	1.00E+01	1.41E-05	3.22E-13	2.11E+01	2.01E+01	2.546000	2.143506	5.155032
3.28E-25	1.21E+01	1.40E-05	3.21E-13	2.19E+01	1.99E+01	2.115643	2.051287	5.213005
2.98E-25	1.19E+01	1.33E-05	3.19E-13	2.12E+01	1.97E+01	2.100458	1.929647	5.264143
2.42E-25	1.19E+01	1.42E-05	3.19E-13	1.99E+01	1.96E+01	1.890210	2.045690	5.309889
2.42E-25	1.08E+01	1.42E-05	3.18E-13	1.97E+01	1.94E+01	1.642900	1.995358	5.351272

Conclusion

In this study we demonstrated the possibility of adding the saccharine quickly to the graphene oxide because it concludes condensation chemical reaction with many other weak forces (van-der Walles and Hydrogen bonding) while the reaction was slowed in the case of graphene because it does not include presence of chemical reaction except through a small number of carboxylic groups not reduced through conversion of GO to G. The infrared spectrum proved that the ratio of saccharin loaded onto the surface and edges of graphene oxide was greater than that loaded onto graphene surface because the height of the peaks was higher in the graphene oxide than graphene. This assignment was confirmed by the measurements of X-ray and conductivity. We observed a large similarity in the diffraction pattern with high conductivity values which were very close to those in the saccharine-graphene. This confirms the possibility of reducing and improving the electrical properties of graphene oxide through add saccharin. As for the speed of storage of energy, the prepared nanomaterials were as follows G-Sac > G > GO-Sac > GO while the speeds of loss were as follows GO > GO-Sac > G > G-Sac. depends on these two series we could conclude that the G-Sac nanomaterial is the best material for rapid charging and lowest loss speed. Also the convergence of the conductivity values and the permittivity parameters of the two compounds containing the saccharin gives a strong and clear evidence that the resulting compounds have a relatively similar structure.

Acknowledgment

The authors would like to thank, Tikrit University for support.

References

[1] Gao, W. (2015). The chemistry of graphene oxide. In *Graphene oxide* (pp. 61-95). Springer, Cham.

[2] Zhang, C., Lei, C., Cen, C., Tang, S., Deng, M., Li, Y., & Du, Y. (2018). Interface polarization matters: Enhancing supercapacitor performance of spinel NiCo2O4 nanowires by reduced graphene oxide coating. *Electrochimica Acta*, *260*, 814-822.

[3] Li, C. Q., Zha, J. W., Li, Z. J., Zhang, D. L., Wang, S. J., & Dang, Z. M. (2018). Towards balanced mechanical and electrical properties of thermoplastic vulcanizates composites via unique synergistic effects of single-walled carbon nanotubes and graphene. *Composites Science and Technology*, *157*, 134-143.

[4] Kumar, S., Wani, M. Y., Arranja, C. T., Castro, R. A., Paixão, J. A., & Sobral, A. J. (2018). Synthesis, physicochemical and optical properties of bis-thiosemicarbazone functionalized graphene oxide. *Spectrochimica Acta Part A: Molecular and Biomolecular Spectroscopy*, *188*, 183-188.

[5] Song, B., Gu, H., Zhu, S., Jiang, H., Chen, X., Zhang, C., & Liu, S. (2018). Broadband optical properties of graphene and HOPG investigated by spectroscopic Mueller matrix ellipsometry. *Applied Surface Science*.

[6] Wang, X., Li, N., Wang, J., Li, G., Zong, L., Liu, C., & Jian, X. (2018). Hyperbranched polyether epoxy grafted graphene oxide for benzoxazine composites: Enhancement of mechanical and thermal properties. *Composites Science and Technology*, *155*, 11-21.

[7] Wang, T., Quinn, M. D., & Notley, S. M. (2018). Enhanced electrical, mechanical and thermal properties by exfoliating graphene platelets of larger lateral dimensions. Carbon, 129, 191-198.

[8] Adak, N. C., Chhetri, S., Kim, N. H., Murmu, N. C., Samanta, P., & Kuila, T. (2018). Static and Dynamic Mechanical Properties of Graphene Oxide-Incorporated Woven Carbon Fiber/Epoxy Composite. *Journal of Materials Engineering and Performance*, *27*(3), 1138-1147.

[9] Bai, S., Jiang, L., Xu, N., Jin, M., & Jiang, S. (2018). Enhancement of mechanical and electrical properties of graphene/cement composite due to improved dispersion of graphene by addition of silica fume. *Construction and Building Materials*, *164*, 433-441.

[10] Panda, S., Rout, T. K., Prusty, A. D., Ajayan, P. M., & Nayak, S. (2018). Electron Transfer Directed Antibacterial Properties of Graphene Oxide on Metals. *Advanced Materials*.

[11] Javanbakht, S., & Namazi, H.(2018). Doxorubicin loaded carboxymethyl cellulose/ graphene quantum dot nanocomposite hydrogel films as a potential anticancer drug delivery system. *Materials Science and Engineering: C*, *87*, 50-59.

[12] Ju, L., Dai, Y., Wei, W., Li, M., Jin, C., & Huang, B. (2018). Theoretical study on the photocatalytic properties of graphene oxide with single Au atom adsorption. *Surface Science*, *669*, 71-78.

[13] Zhu, X. Y., Lv, Z. S., Feng, J. J., Yuan, P. X., Zhang, L., Chen, J. R., & Wang, A. J. (2018). Controlled fabrication of well-dispersed AgPd nanoclusters supported on reduced graphene oxide with highly enhanced catalytic properties towards 4-nitrophenol reduction. *Journal of Colloid and Interface Science*.

[14] Qian, Y., Ismail, I. M., & Stein, A. (2014). Ultralight, high-surface-area, multifunctional graphene-based aerogels from self-assembly of graphene oxide and resol. *Carbon*, *68*, 221-231.

[15] Pei, S., Wei, Q., Huang, K., Cheng, H. M., & Ren, W. (2018). Green synthesis of graphene oxide by seconds timescale water electrolytic oxidation. *Nature communications*, *9*(1), 145.

[16] Hong, Y. Z., Tsai, H. C., Wang, Y. H., Aumanen, J., Myllyperkiö, P., Johansson, A., & Woon, W. Y. (2018). Reduction-oxidation dynamics of oxidized graphene: Functional group composition dependent path to reduction. *Carbon*, *129*, 396-402.

[17] Gao, W. (2015). The chemistry of graphene oxide. In *Graphene oxide* (pp. 61-95). Springer, Cham.

[18] Zhu, Y., Murali, S., Cai, W., Li, X., Suk, J. W., Potts, J. R., & Ruoff, R. S. (2010). Graphene and graphene oxide: synthesis, properties, and applications. *Advanced materials*, *22*(35), 3906-3924..

[19] Abd, A. N., Al-Agha, A. H., Alheety, M. A. (2016). Addition of Some Primary and Secondary Amines to Graphene Oxide, and Studying Their Effect on Increasing its Electrical Properties. *Baghdad Science Journal*, (1)13, 97-112.

[20] Compton, O. C., Dikin, D. A., Putz, K. W., Brinson, L. C., & Nguyen, S. T. (2010). Electrically conductive "alkylated" graphene paper via chemical reduction of amine-functionalized graphene oxide paper. *Advanced materials*, *22*(8), 892-896.

[21] Lai, L., Chen, L., Zhan, D., Sun, L., Liu, J., Lim, S. H., Poh, C.K., Shen, Z. & Lin, J. (2011). One-step synthesis of NH_2-graphene from in situ graphene-oxide reduction and its improved electrochemical properties. *Carbon*, *49*(10), 3250-3257.

[22] Lu, Y., Zhang, F., Zhang, T., Leng, K., Zhang, L., Yang, X., Ma,Y., Huang, Y. Zhang,M. & Chen, Y. (2013). Synthesis and supercapacitor performance studies of N-doped graphene materials using o-phenylenediamine as the double-N precursor. *Carbon*, *63*, 508-516.

[23] Ai, W., Liu, J. Q., Du, Z. Z., Liu, X. X., Shang, J. Z., Yi, M. D. & Huang, W. (2013). One-pot, aqueous-phase synthesis of graphene oxide functionalized with heterocyclic groups to give increased solubility in organic solvents. *RSC Advances*, *3*(1), 45-49.

[24] Zhai, L., Li, L., & Zhang, Q. (2018). Fabrication of capsaicin functionalized reduced graphene oxide and its effect on proliferation and differentiation of osteoblasts. *Environmental toxicology and pharmacology*, *57*, 41-45.

[25] Vineh, M. B., Saboury, A. A., Poostchi, A. A., Rashidi, A. M., & Parivar, K. (2018). Stability and activity improvement of horseradish peroxidase by covalent immobilization on functionalized reduced graphene oxide and biodegradation of high phenol concentration. *International journal of biological macromolecules*, *106*, 1314-1322.

[26] Du, W., Wu, M., Zhang, M., Xu, G., Gao, T., Qian, L., Yu, X., Chi, F., Li, C. and Shi, G. (2018). High-quality graphene films and nitrogen-doped organogels prepared from the organic dispersions of graphene oxide. *Carbon*, *129*, 15-20.

[27] Chen, H., Müller, M. B., Gilmore, K. J., Wallace, G. G., & Li, D. (2008). Mechanically strong, electrically conductive, and biocompatible graphene paper. *Advanced Materials*, *20*(18), 3557-3561.

[28] Chen, T., Zeng, B., Liu, J., Dong, J., Liu, X., Wu, Z., Yang, X. and Li, Z .(2009). High throughput exfoliation of graphene oxide from expanded graphite with assistance of strong oxidant in modified hummers method . In Journal of physics: conference series.

[29] Xiong, X., Huang, B., Wei, X., Wang, L., & Zhang, L. (2018). Research of Graphene Preparation Methods. In Applied Sciences in Graphic Communication and Packaging. Springer, Singapore., pp. 963-971.

[30] Sewall, L. M.(2006). Dielectric characterization: A 3D EM simulation approach (Doctoral dissertation, Virginia Tech).

[31] Stoyan J., Clark, J., Clark, H.M., Cooper, D., & Cullerne, J. (2006). Dictionary of physics 6thed. Oxford University, UK.press

[32] Singh, V., Joung, D., Zhai, L., Das, S., Khondaker, S. I., & Seal, S. (2011). Graphene based materials: past, present and future. *Progress in materials science*, 56(8), 1178-1271.

[33] Krishnan, M. A., Aneja, K. S., Shaikh, A., Bohm, S., Sarkar, K., Bohm, H. M., & Raja, V.S.

(2018). Graphene-based anticorrosive coatings for copper. *RSC Advances*, *8*(1), 499-507.
[34] Ahmadzadeh, M., Zarnegar, Z., & Safari, J. (2018). Sonochemical synthesis of methyl-4-(hetero) arylmethylene isoxazole-5 (4 H)-ones using SnII-montmorillonite. *Green Chemistry Letters and Reviews*, *11*(2), 78-85.
[35] Singu, D. C., Joseph, B., Velmurugan, V., Ravuri, S., & Grace, A. N. (2018). Combustion Synthesis of Graphene from Waste Paper for High Performance Supercapacitor Electrodes. *International Journal of Nanoscience*, *17*(01n02), 1760023.
[36] To, S. S., Wang, V. H., & Lee, W. B. (2018). Materials Deformation Behaviour and Characterisation. In Materials Characterisation and Mechanism of Micro-Cutting in Ultra-Precision Diamond Turning. Springer, Berlin, Heidelberg, pp. 71-104.
[37] Li, X., Liu, W., Sun, L., Aifantis, K. E., Yu, B., Fan, Y., Feng, Q., Cui, F., & Watari, F. (2014). Resin composites reinforced by nanoscaled fibers or tubes for dental regeneration. *BioMed research international*, *2014*.

تحضير وتشخيص ودراسة مقارنة للخصائص الكهربائية لاوكسيد الكرافين والكرافين بعد تحميل مادة محليه صناعية عليهما (السكارين)

فراس سعيد عبد العزيز، ابتهال قحطان عبدالله ، مصطفى عبد الغفور
قسم الكيمياء ، كلية العلوم ، جامعة تكريت ، تكريت ، العراق

الملخص

تم تحضير اثنين من هياكل الكربون النانوية هما أوكسيد الكرافين (GO) والكرافين (G) بهدف دراسة خواصهما الكهربائية بعد توظيفهما مع السكارين. بعد تحضير أوكسيد الكرافين المكلور تم ربط السكارين بشكل تساهمي مع بنية أوكسيد الكرافين النانوية وتكوين اصرة امايدية لـ (GO-Sac)، كما تم ربط السكارين فيزيائياً برقائق الكرافين النانوية وتكوين (G-Sac). تم تشخيص هذين المشتقين بأستخدام تقنية (FT-IR)، حيود الاشعة السينية (XRD) وتقنية المجهر الذري (AFM). هنا لا يستخدم السكارين فقط لتحسين الخصائص الكهربائية لاوكسيد الكرافين (GO) والكرافين (G) ولكنه لعب دوراً رئيساً في زيادة المسافة بين صفائح أوكسيد الكرافين والمسافة بين صفائح الكرافين أيضا وبالتالي منع تأثير التكتل على صفائحهما. تم قياس الخواص الكهربائية لهذه المواد باستخدام معامل الحث، السعة وقياس المقاومة (LCR) واظهرت النتائج زيادة الخصائص الكهربائية لمركبي الكربون النانوية مع تحسين التخزين الكهربائي بعد المعالجة بالسكارين.